Hindawi
Geofluids
Volume 2022, Article ID 3241211, 10 pages
https://doi.org/10.1155/2022/3241211

Research Article

Numerical Optimization of Drilling Parameters for Gas Predrainage and Excavating-Drainage Collaboration on Roadway Head

Mingkun Luo,[1,2,3] Lei Yang,[1] Haiou Wen,[1] Dongsheng Zhao,[2] and Kun Wang[2]

[1]*College of Mining, Liaoning Technical University, Fuxin, Liaoning 123000, China*
[2]*Zhangcun Coal Mine, Shanxi Lu'an Chemical (Group) Co., Ltd, Changzhi, Shanxi 046299, China*
[3]*Institute of Science and Technology, Shanxi Lu'an Chemical (Group) Co., Ltd, Changzhi, Shanxi 046299,), China*

Correspondence should be addressed to Lei Yang; leiyang106@163.com

Received 9 November 2021; Accepted 14 December 2021; Published 20 May 2022

Academic Editor: Liang Xin

In order to improve efficiency of gas drainage, the reasonable layout parameters for borehole on roadway head are investigated. Assuming that the coal mass has a dual pore structure with fractures and pores, a multiphysical field coupling mathematical model is proposed for gas drainage. The governing equations of gas adsorption, seepage, and diffusion are considered. The process of gas preextraction and excavating-extraction collaboration on roadway heading face in 2606 haulage roadway of Zhangcun mine is modeled by finite element (FE) method. The effects of gas drainage under different drilling arrangements are analyzed. The results show that the fastest decreasing rate of gas content occurs at the beginning of drainage, and decreasing rate of gas content tends to be stable in the later stage. After removing the predraining on roadway head, the gas content at the center of coal wall on the roadway heading face will rebound. The included angle between the borehole and the roadway middle line determines the spatial area of gas drainage. Too small included angle will reduce the area of gas content reduction, while too large included angle will result in a blind area on both sides of the roadway. The change in borehole spacing affects the decreasing rate of gas content in the rock and coal around the roadway. Large spacing may cause an inadequate decreasing rate in the middle of the roadway, while small spacing may cause an inadequate decreasing rate in both sides of the roadway. In the field application, the pure gas flow and gas concentration of drainage show a downward trend in whole. The gas concentration decreased from 13.2% to 10.8%, and the pure gas flow decreased from 10.6 m^3/min to 8.15 m^3/min. Research achievements can provide a basis for gas drainage in underground roadway.

1. Introduction

Coal mine gas is the main harm of coal production, it is also a kind of clean energy [1]. As the depth of mining increases, the permeability of coal seams decreases gradually [2, 3]. In this case, the danger and intensity of coal and gas outburst are increasing [4]. Underground gas drainage is the main method to reduce gas content and prevent gas disasters [5, 6]. Therefore, studying the seepage law and reasonable drilling layout parameters during gas drainage is of vital meaning for effective gas predrainage and reducing engineering costs.

Predecessors have done a lot of research on the seepage law during gas drainage. Wu [7] proposed a gas-coal coupling model based on the interaction among gas diffusion, seepage, and coal deformation. Yin et al. [8, 9] considered the Klinkenberg effect and ab/desorption induced strain effect to establish a gas-solid mathematic model and perform numerical simulations with the aid of finite elements. Zhang et al. [10] obtained the porosity and permeability equations with adsorption caused deformation. According to the gas seepage characteristics and dynamic change in coal permeability, Liang et al. [11] studied the gas seepage processes in fracture, microporous adsorption gas desorption and diffusion, and deformation of coal and rock mass and established a couple seepage model. Lin et al. [12] established a multiphysics coupled model of diffusion, stress, and seepage

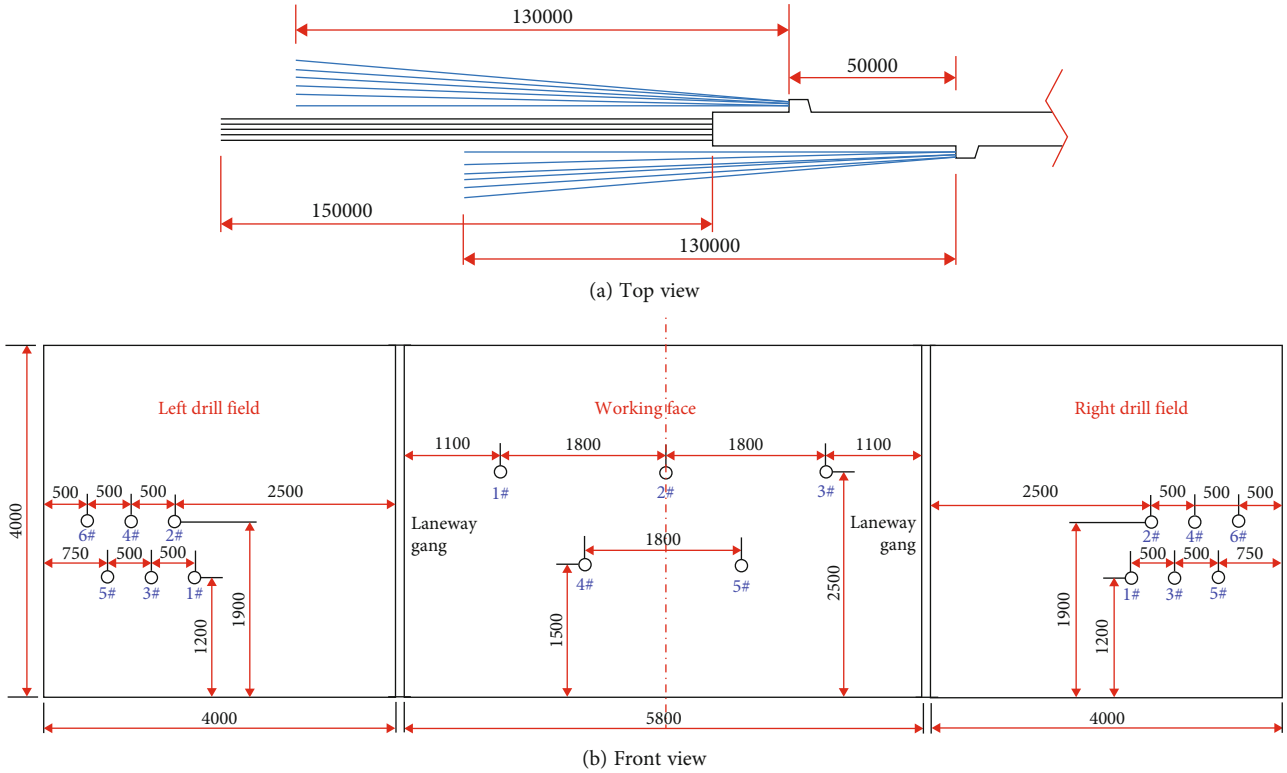

Figure 1: Schematic diagram of the layout of the 2606 haulage roadway of gas preextraction and excavating extraction collaboration.

fields and introduced the dynamic diffusion coefficient to explore the seepage evolution during gas drainage. In addition, some scholars have studied the desorption and adsorption behavior of coal at the microscopic level [13, 14] and the influence of polymer on coal desorption and adsorption [15]. For the borehole spacing, too small spacing will increase the amount of work in the drilling construction and rise the instability risk of drilling such as pierce or collapse holes resulting from the pressure relief damage of coal and rock, while too large spacing will leave blind area of drainage, which not only can hardly eliminate the outbursts but also aggravate the hidden dangers of gas accidents [16]. To this end, scholars have launched a study on the extraction radius. Zhang et al. [17] used a self-developed device to conduct experimental research on different drilling arrangements and explored the extraction radius when the drilling holes interact with each other. Lin et al. [18] studied the effect of the adsorption constant on the extraction radius through numerical simulations. Qin et al. [19] obtained reasonable drainage parameters through the study of drainage radius. These provide a reference for numerical simulation and engineering practice of underground gas drainage.

However, there are few studies for gas predrainage and excavating-drainage collaboration on roadway head. This paper is based on the assumption of dual porosity and single permeability and comprehensively considers the gas slippage effect, effective stress, and deformation characteristics of coal seam, and a multiphysics coupled model composed of fluid migration, coal deformation under stresses, and gas diffusion controlling equations is established. This mathematical model was embedded in the FE software-COMSOL Multiphysics, to simulate gas drainage law of the 2606 haulage roadway in Zhangcun Mine. The processes of gas predrainage and excavating-drainage collaboration on roadway head under different schemes were simulated. The research results can provide guidance for optimizing of drainage boreholes layout.

2. Coal Seam Gas Drainage Mathematical Model

2.1. General Hypothesis. Based on the general law of gas transport within coal seam and related literatures [20–23], some hypotheses are proposed: (1) coal and rock mass has a dual pore structure composed with pores-fractures. (2) Gas diffusion in the pore system of coal matrix follows Fick's law, and gas seepage in fracture system follows Darcy's law. (3) Water only moves in the fractures. (4) Ignore the influence of coal seam temperature on gas drainage. (5) Gas is regarded as an ideal gas. (6) The tensile stress is positive.

2.2. Permeability Evolution Model. According to hypothesis, the matrix porosity model can be obtained [24]:

$$\varphi_m = \frac{(1+S_0)\varphi_{m0} + \alpha_m(S-S_0)}{(1+S)}, \tag{1}$$

where φ_{m0} is the original matrix porosity; $\alpha_m = 1 - K/K_s$ is the Biot's coefficient for matrix; K is the bulk modulus of coal, GPa; $K_s = E_s/3(1-2v)$ is the bulk modulus of coal skeleton, GPa; E_s is the elastic modulus of coal skeleton, GPa; v is the Poisson's ratio of coal; $S = \varepsilon_v + p_{mg}/K_s - \varepsilon_a$ is the

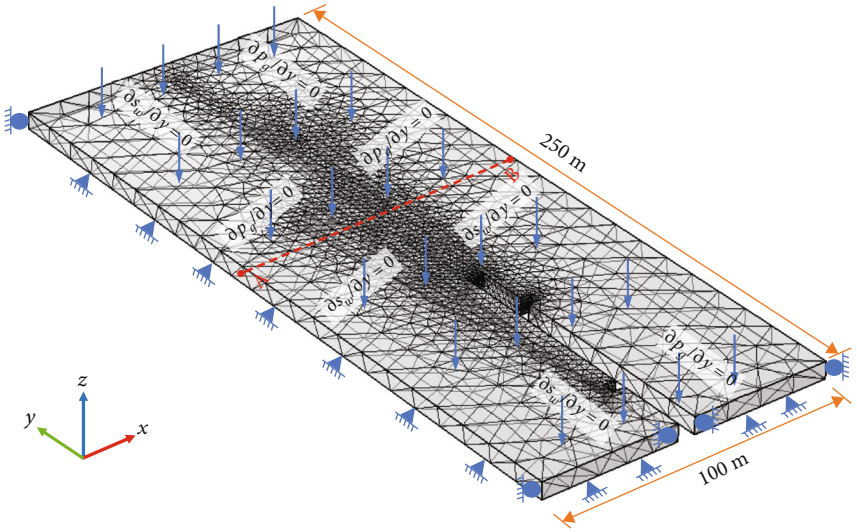

Figure 2: Numerical simulation of physical geometry model.

matrix porosity strain; ε_v is the volumetric strain; the term "0" stands the original value.

The relationship between adsorbed gas strain of coal skeleton and the adsorbed amount can be expressed as follows [25]:

$$\varepsilon_a = \alpha_{\mathrm{sg}} V_{\mathrm{sg}}, \tag{2}$$

where α_{sg} is the sorption induced strain factor, kg/m^3; V_{sg} is the adsorbed gas content, m^3/kg.

Based on the modified Langmuir equation, the adsorbed gas content may be expressed by the following [26]:

$$V_{\mathrm{sg}} = \frac{V_L p_{\mathrm{mg}}}{P_L + p_{\mathrm{mg}}}, \tag{3}$$

where V_L and P_L are the Langmuir constants; p_{mg} is gas pressure in coal matrix, MPa.

The fracture porosity model is as follows [27]:

$$\varphi_f = \varphi_{f0} - \frac{3\varphi_{f0}}{\varphi_{f0} + 3K_f/K}[(\varepsilon_a - \varepsilon_{a0}) - (\varepsilon_v - \varepsilon_{vo})], \tag{4}$$

where φ_{f0} is the original fracture porosity; $K_f = qK_n$ is the effective stiffness, GPa; q is the fracture width, m; K_n is fracture stiffness, GPa/m.

The permeability of fracture can be obtained by cubic law [28]:

$$k = k_0 \cdot \left(\frac{\varphi_f}{\varphi_{f0}}\right)^3 = k_0 \left\{1 - \frac{3}{\varphi_{f0} + 3K_f/K}[(\varepsilon_a - \varepsilon_{a0}) - (\varepsilon_v - \varepsilon_{vo})]\right\}^3, \tag{5}$$

where k_0 is the origin permeability, m^2.

The relative permeabilities are set to illustrate the gas and water transport speed in two-phase flow, which are derived as follows [29]:

$$\begin{cases} k_{\mathrm{rg}} = k_{\mathrm{rg0}}\left[1 - \left(\dfrac{s_w - s_{wr}}{1 - s_{\mathrm{wr}} - s_{\mathrm{gr}}}\right)\right]^2\left[1 - \left(\dfrac{s_w - s_{\mathrm{wr}}}{1 - s_{\mathrm{wr}}}\right)^2\right], \\ k_{\mathrm{rw}} = k_{\mathrm{rw0}}\left(\dfrac{s_w - s_{\mathrm{wr}}}{1 - s_{\mathrm{wr}}}\right)^4, \end{cases} \tag{6}$$

where k_{rg0} is gas endpoint permeability; s_w is water saturation; s_{wr} is bound water saturation; s_{gr} is residual gas saturation; k_{rw0} is water endpoint permeability.

2.3. Seepage Field Controlling Equation

2.3.1. Gas Transport in Matrix. Gas mass in one unit coal matrix contains both free and adsorbed components [30]:

$$m_m = \varphi_m \rho_g + V_{\mathrm{sg}} \rho_c \rho_{\mathrm{gs}}, \tag{7}$$

where ρ_s is the density of coal skeleton, kg/m^3; ρ_{gs} is gas density under standard conditions, kg/m^3.

Satisfying the ideal gas law, the gas density can be obtained as follows:

$$\rho_g = \frac{M_g}{RT} p, \tag{8}$$

where M_g is the gas molar mass, g/mol; R is the gas mole constant, J/(mol·K); p is the pressure, MPa; T is coal temperature, K.

Due to the effect of drainage breaking the dynamic balance in gas ad/desorption in coal seams, the free gas in matrix pores diffuses into coal fracture caused by the

Table 1: Numerical simulation parameters.

Parameter	Value	Parameter	Value
Initial CH_4 pressure (p_0, MPa)	0.80	Gas sorption time CH_4 (τ, d)	4.34
Young's modulus of coal seam (E, MPa)	3500	Coal density (ρ_c, kg·m^{-3})	1380
Young's modulus of skeleton (E_s, MPa)	8469	Klinkenberg factor (b, MPa)	0.62
Poisson's ratio of coal (ν)	0.30	Original temperature (T, K)	289.15
Langmuir volume constant of CH_4 (V_L, m^3·kg^{-1})	0.0323	Matrix initial porosity (φ_{m0})	0.04
Langmuir pressure constant of CH_4 (P_L, MPa)	2.0833	Initial porosity of fracture (φ_{f0})	0.018
Initial permeability (k_0, m^2)	2.56×10^{-17}	Residual gas saturation (s_{gr})	0.15
Dynamic viscosity of water (μ_w, Pa·s)	1.01×10^{-3}	Initial water saturation (s_{w0})	0.6
Dynamic viscosity of CH_4 (μ_{g1}, Pa·s)	1.03×10^{-5}	Irreducible water saturation (s_{wr})	0.42

Table 2: Drilling layout parameters of different schemes.

	Borehole order	Predrainage					Excavating drainage					
		1#	2#	3#	4#	5#	1#	2#	3#	4#	5#	6#
Scheme one	Angle between borehole and middle line of the roadway/°	0	0	0	0	0	0	1	2	4	6	7
	Drilling spacing/m			1.8					0.5			
Scheme two	Angle between borehole and middle line of the roadway/°	0	0	0	0	0	0	0	0	0	0	0
	Drilling spacing/m			1.8					0.5			
Scheme three	Angle between borehole and middle line of the roadway/°	0	0	0	0	0	1	3	5	7	9	11
	Drilling spacing/m			1.8					0.5			
Scheme four	Angle between borehole and middle line of the roadway/°	0	0	0	0	0	0	1	2	4	6	7
	Drilling spacing/m			1.3					0.1			
Scheme five	Angle between borehole and middle line of the roadway/°	0	0	0	0	0	0	1	2	4	6	7
	Drilling spacing/m			2.3					0.9			

concentration difference. The gas balance in coal matrix can be derived from Fick's diffusion law. For [28],

$$\frac{\partial m_m}{\partial t} = -\frac{M_g}{\tau RT}\left(p_{\mathrm{mg}} - p_{\mathrm{fg}}\right), \tag{9}$$

where τ is the gas sorption time, s; p_{fg} is the fracture pressure, MPa.

Combining Equations (3) and (7)–(9), the controlling equation for gas migration in coal matrix is gained.

$$\frac{\partial}{\partial t}\left(\varphi_m \frac{M_g}{RT} p_{\mathrm{mg}} + \frac{V_L p_{\mathrm{mg}}}{p_L + p_{\mathrm{mg}}} \rho_c \frac{M_g}{RT} p_a\right) = -\frac{M_g}{\tau RT}\left(p_{\mathrm{mg}} - p_{\mathrm{fg}}\right). \tag{10}$$

2.3.2. Fluid Migration within Fractures. The modified Darcy's law is adopted to govern the fluid flow of gas and water in fractures [31]:

$$\begin{cases} q_g = -\dfrac{kk_{\mathrm{rg}}}{\mu_g}\left(1 + \dfrac{b}{p_{\mathrm{fg}}}\right)\nabla p_{\mathrm{fg}}, \\ q_w = -\dfrac{kk_{\mathrm{rw}}}{\mu_w}\nabla p_{\mathrm{fw}}, \end{cases} \tag{11}$$

where b is the Klinkenberg factor, MPa; k_{rw} is water relative permeability; k_{rg} is gas relative permeability; μ_w is the dynamic viscosity of water, Pa·s; μ_g is the dynamic viscosity of gas, Pa·s.

The gas-water balance equations in the fracture are expressed as follows [32]:

$$\begin{cases} \dfrac{\partial}{\partial t}\left(s_g \varphi_f \dfrac{M_g}{RT} p_{\mathrm{fg}}\right) - \nabla \cdot \left(\dfrac{M_g}{RT} \dfrac{kk_{\mathrm{rg}}\left(p_{\mathrm{fg}} + b\right)}{\mu_g} \nabla p_{\mathrm{fg}}\right) = \left(1 - \varphi_f\right) \dfrac{M_g}{\tau RT}\left(p_{\mathrm{mg}} - p_{\mathrm{fg}}\right), \\ \dfrac{\partial\left(s_w \varphi_f \rho_w\right)}{\partial t} - \nabla \cdot \left(\dfrac{\rho_w k k_{rw}}{\mu_w} \nabla p_{\mathrm{fw}}\right) = 0, \end{cases} \tag{12}$$

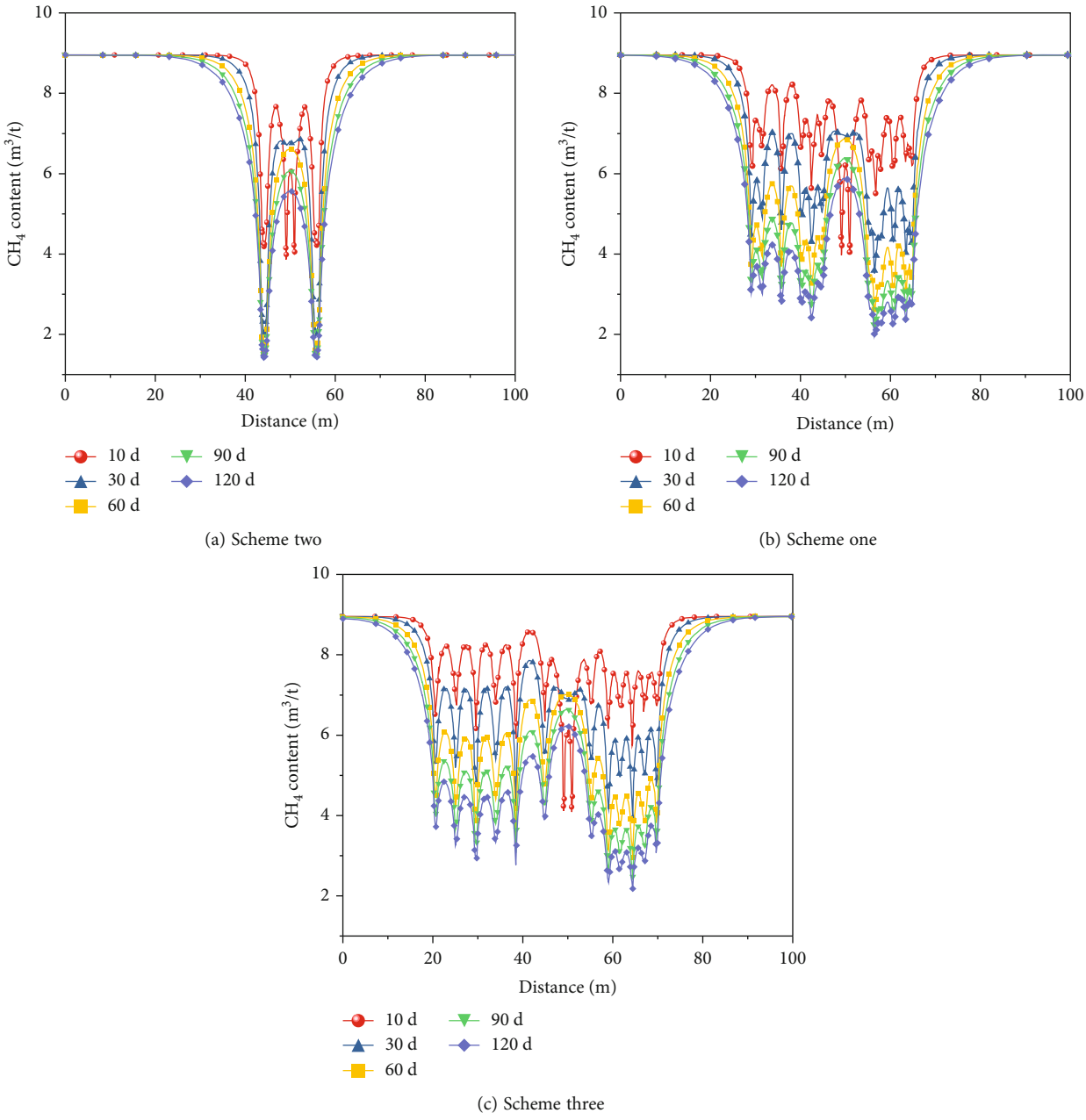

(a) Scheme two

(b) Scheme one

(c) Scheme three

Figure 3: Evolution curve of gas content on reference line AB under different arrangements of included angle.

where s_g means gas saturation and ρ_w means water density, kg/m^3.

2.4. Stress Field Controlling Equation. The deformation of coal seam concludes solid stress caused strain, gas and water pressure caused strain, and gas sorption induced strain. The controlling equation for coal stress-strain field is as follows [33]:

$$Gu_{i,jj} + \frac{G}{1-2\nu} u_{j,ji} - \alpha_m p_{m,i} - \alpha_f p_{f,i} - K\varepsilon_{a,i} + F_i = 0, \quad (13)$$

where G is the shear modulus of coal, GPa; p_f is the fluid pressure in fractures, Pa; F_i is the volume force, GPa; α_f is the Biot's coefficient for fracture.

3. Physical Model and Solution Settings

3.1. Studied Case. Zhangcun Coal Mine is situated at the eastern edge of Qinshui Basin in Shanxi Province. The regional stratigraphic division belongs to the stratigraphic community in the southern section of Taihang Mountain in the Shanxi stratigraphic division. The stratum generally moves in the NNE direction, dipping gently to W, with an inclination angle of 5-15°. Lane 2606 is located on the north side of lane 26, 300 m away from lane 2605 in the east. The ground elevation of the excavation area is about +972 ~ +992 m. The cross-section of the roadway is 5.8 × 4.0 m (width × height) rectangle with a cross-sectional area of 23.2 m^2. The mined seam belongs to No. 3 coal seam in

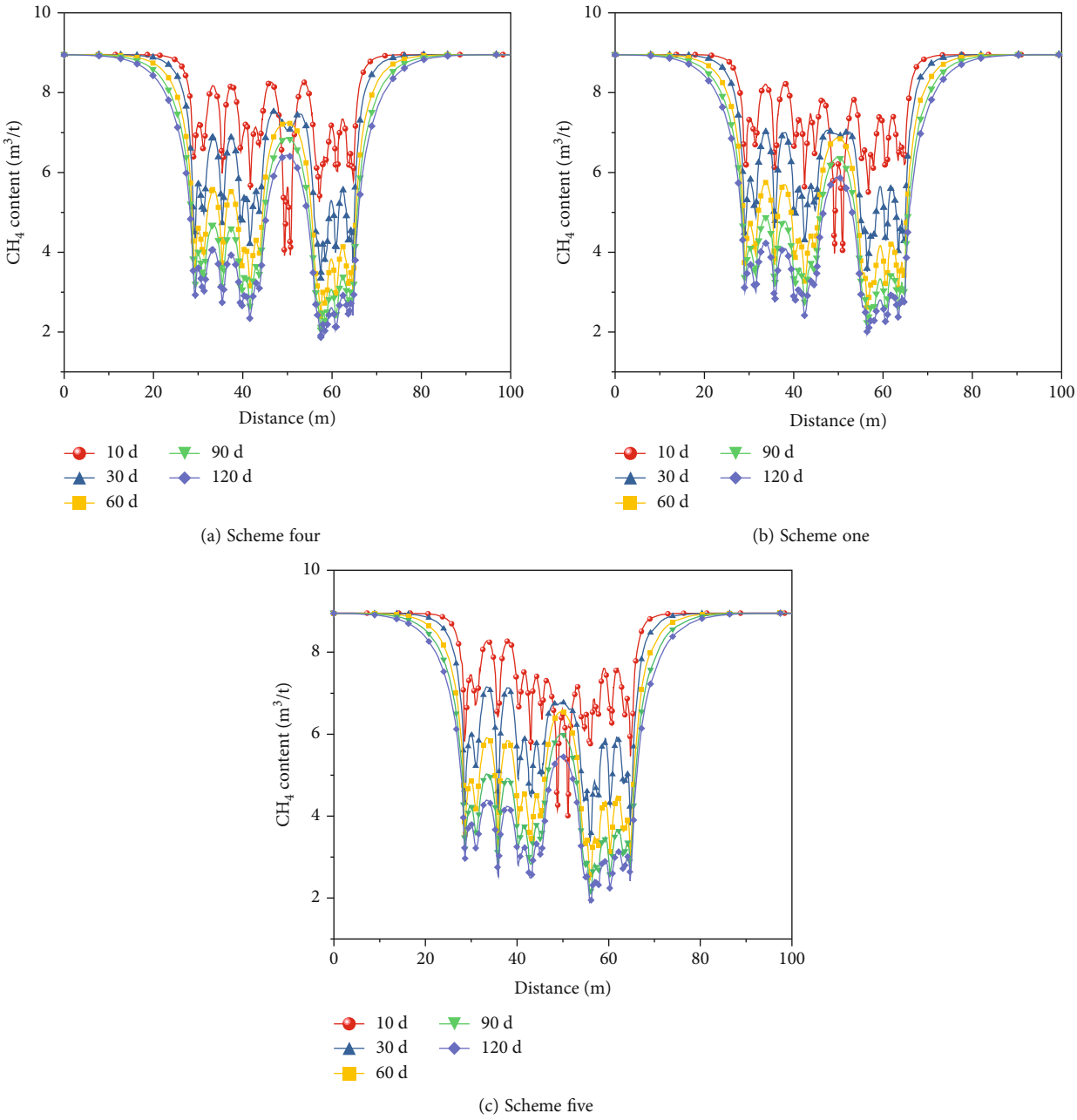

Figure 4: Evolution curve of gas content on reference line A-B under different borehole spacing.

the Shanxi Formation. The coal seam is stable, with less variation in coal thickness and simpler coal seam structure. The buried depth is about 537 m, and the thickness is 5.33 m-6.19 m, and the average thickness is 5.86 m. The original gas content during the 2606 roadway driving period is 8.5-10.0 m^3/t, and the coal seam temperature is 15°C-17°C. During the excavating process, the mining depth continued to increase, and the gas content for 3# coal seam showed an increasing trend.

Therefore, gas preextraction and excavating extraction collaboration were adopted to ensure the safe operation of the 2606 roadway during excavation. During the excavating period, the gas predraining is carried out every 130 m. The gas predraining is arranged head-on with 5 drilling holes on the working face. Drilling length is 150 m, and the safety distance is 20 m. The method of excavating extraction is to arrange the stepping drill field in the roadway at a step distance of 50 m (the same side drill field spacing is 100 m). The stepping drilling field is arranged, and each stepping drilling field is arranged with 6 holes, and the drilling depth is 130 m. The layout of the 2606 haulage roadway of gas preextraction and excavating extraction is shown in Figure 1.

3.2. Physical Model and Definite Solution Conditions. According to 2606 roadway gas extraction scheme, the physical geometric model as shown in Figure 2 is established. And through the simulation results obtained after changing spacing and angle of the boreholes, determine the best

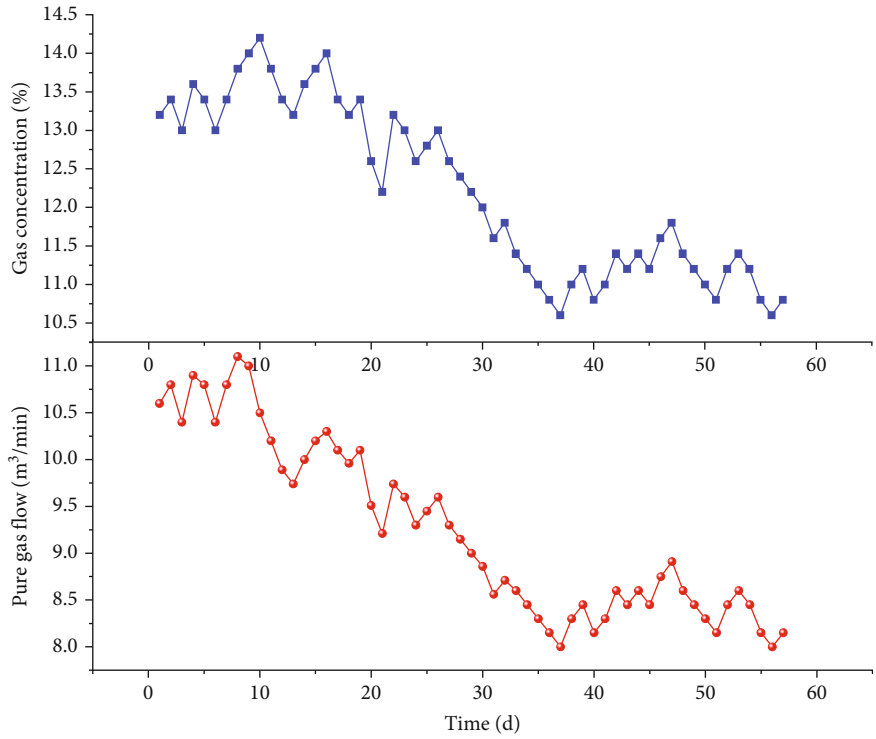

Figure 5: 2606 roadway gas concentration and pure gas flow change.

scheme for gas drainage on 2606 haulage roadway of Zhangcun Coal Mine. The reference line A-B in the physical model is set to see the changes in gas content. The initial gas pressure is 0.8 MPa, the overburden gravity of 14.85 MPa in the z direction is applied of the model, and roller bearing boundary conditions are set around the model. The bottom boundary is fixed. The outer boundaries of the model are impermeable. The diameter of the borehole is 94 mm, and the negative pressure for gas drainage is 20 kPa. The other used parameters are shown in Table 1, which are derived from literature [33] and field data.

4. Analysis of Numerical Simulation

4.1. Different Scheme Design. To determine a reasonable drainage drilling arrangement scheme and obtain the best drainage effect. By changing the borehole spacing and the angle, the following five schemes were formulated up for the 2606 haulage roadway gas drainage in Zhangcun Coal Mine, and using the FE software COMSOL Multiphysics, the gas drainage effect of these schemes is analyzed. The drainage schemes are shown in Table 2.

4.2. Evolution of Gas Content under Different Schemes. In order to ensure the extraction progress of 2606 haulage roadway, the head predrainage after 10 days of drainage will be canceled. In Figure 3, gas content on the reference line A-B under different borehole arrangement angles shows decrease trend as extraction time prolongs. The fastest decrease rate of gas content occurs in the initial stage of drainage. As gas pressure in coal seam decreases, the gas flow decreases, so the decrease rate of gas content tends to be stable in the later stage. Comparing Figures 3(a) and 3(b), the decrease rate of gas content in schemes 1 and 2 is basically the same near on the roadway middle line. However, the area of gas content decrease is different. Scheme 1 has a greater impact within 22 m around the roadway middle line, and scheme 2 has a greater impact within 9 m around the roadway middle line. The borehole is drilled at an angle to the roadway middle line in scheme 1, which covers wider area on both sides of the roadway. And the included angle between the borehole and the roadway middle line is 0° in scheme 2. Therefore, the spatial area of influence of the first scheme is larger than that of the second scheme. From Figure 3(c), compare scheme 3 and scheme 1, although the angle between the borehole and the roadway middle line becomes larger, and gas content decrease area is increases, but the overall decrease rate of gas content in scheme 3 is slowed down. The most important thing is that with the extension of the boreholes, the angle between the boreholes in scheme 3 gradually increases, and drainage blind areas appear, causes the gas content to decrease slowly (as can be seen in the 7 m area on the left side of the middle line of the roadway in Figure 3(c)), and the ideal drainage effect cannot be achieved. After removing the predrainage on roadway head, the gas content at the middle line of coal wall on the roadway heading face will rebound. The gas content in the roadway middle line is relatively lower than the gas content of the roadway two flanks after 10 d for gas predrainage and excavating-drainage collaboration on roadway head. When there is a pressure gradient, the gas in the roadway two sides will move to the direction of the roadway middle line. At this time, the gas content in the roadway middle line will rise.

As can be seen from Figure 4. The change of the borehole spacing has a weak influence on the drainage area. However, this affects the gas content decreasing rate in the rock and coal around the roadway. Comparing Figures 4(a) and 4(b), in scheme 4, the peak gas content within 5 m on the roadway middle line after 10, 30, 60, 90, and 120 days of drainage is 8.3 m^3/t, 7.6 m^3/t, 7.3 m^3/t, 6.9 m^3/t, and 6.4 m^3/t, respectively. The peak gas content within 5 m on the roadway middle line in scheme 1 is 7.8 m^3/t, 7.0 m^3/t, 6.8 m^3/t, 6.4 m^3/t, and 5.9 m^3/t, respectively. Compared with scheme 4, the gas content of roadway two sides decreases faster in scheme 1, while the gas content of the roadway both sides decreases slowly, and as a result, the gas content of the scheme 4 rises more than the scheme 1 of the coal wall on the roadway heading face. From Figures 4(b) and 4(c), in the case of 10 days of gas predrainage and excavating drainage collaboration on roadway head, the gas content peak on the roadway midline line in scheme 5 is 6.6 m^3/t, and the gas content peak on the roadway midline line the in scheme 1 is 6.1 m^3/t. The gas content of the scheme 1 drops faster than that of the scheme 5 on the roadway middle line in the early stage.

From the above analysis, the too small included angle between the borehole and the roadway middle line results the spatial area of gas content decrease, it not only can hardly achieve the desired drainage effect but also may increase engineering costs. When the too large angle between the borehole and the roadway middle line will result a blind area for drainage on the roadway of two sides, spacing of borehole is too small, and the results lower the decrease rate of gas content on the roadway two sides. Spacing of borehole is too large, which caused an inadequate decreasing rate of gas content on the roadway middle line, and the drainage effects of both are poor. Therefore, in general, among the five gas drainage schemes designed for the 2606 haulage roadway of Zhangcun Coal Mine, scheme 1 is the best drainage effect.

5. Field Applications

According to the simulation of gas combined drainage on 2606 haulage roadways in Zhangcun Coal Mine. It is preliminarily determined that the spacing of the preextraction boreholes at the front end of the 2606 haulage roadway is 1.8 m. The distance between the excavating extraction boreholes is 0.5 m, and the angles between borehole and middle line of the roadway are 0°, 1°, 2°, 4°, 6°, and 7°. The boreholes are connected to the pipe network for drainage. The gas drainage concentration and drainage volume monitored during the period are shown in Figure 5.

After nearly 2 months of drainage, the gas concentration and drainage of pure quantity around the 2606 haulage roadway have significantly decreased trend, and the drainage effect is ideal. The gas concentration decreased from 13.2% to 10.8%, a decrease of 18.2%. And the pure gas flow decreased from 10.6 m^3/min to 8.15 m^3/min, a decrease of 23.1%. Results show that it is feasible to adopt scheme 1 as the gas drainage plan during the 2606 roadway excavation period.

6. Conclusions

(1) Considering that the coal mass is a dual porous structure, a multiphysics coupling mathematical model of coal seam gas drainage was established involving gas sorption, diffusion, and seepage. The COMSOL Multiphysics software is used to simulate gas predrainage and excavating-drainage collaboration on roadway head

(2) The process of gas drainage with different borehole arrangements in 2606 roadway in Zhangcun Coal Mine is simulated. The results show that the fastest decreasing rate of gas content occurs in the initial stage of drainage, and the decreasing rate of gas content tends to be stable in the later stage. After removing the predraining on roadway head, the gas content at the center of coal wall on the roadway heading face will rebound

(3) The included angle between the borehole and roadway middle line determines the spatial area of gas drainage. Too small included angle will reduce the area of gas content reduction, while too large included angle will result in a blind area on both sides of the roadway. The change in borehole spacing affects the decreasing rate of gas content in the coal wall around the roadway. Large spacing may cause an inadequate decreasing rate in the middle coal wall of the roadway, while small spacing may cause an inadequate decreasing rate in both sides of the roadway

(4) Gas drainage is carried out in 2606 haulage roadway of Zhangcun Coal Mine. After nearly 2 months of drainage, gas concentration decreased from 13.2% to 10.8%, with a decrease of 18.2%. And the pure gas flow decreased from 10.6 m^3/min to 8.15 m^3/min, with a decrease of 23.1%. The pure gas flow and gas concentration of drainage show a downward trend in whole which matches the results of numerical simulations

Data Availability

Experimental data used to support the findings of this study are included within the article

Conflicts of Interest

The authors declare no conflicts of interest.

Acknowledgments

This research was financially supported by the project supported by the Postdoctoral Science Foundation of China (Grant No. 2018 M641675).

References

[1] C. J. Fan, S. Li, D. Elsworth, J. Han, and Z. H. Yang, "Experimental investigation on dynamic strength and energy

dissipation characteristics of gas outburst prone coal," *Energy Science & Engineering*, vol. 8, no. 4, pp. 1015–1028, 2020.

[2] L. L. Si, J. P. Wei, Y. J. Xi et al., "The influence of long-time water intrusion on the mineral and pore structure of coal," *Fuel*, vol. 290, no. 1, article 119848, 2021.

[3] Z. J. Zhu, Y. L. Wu, and J. Han, "A Prediction Method of Coal-Burst Based on Analytic Hierarchy Process and Fuzzy Comprehensive Evaluation," *Frontiers in Earth Science*, vol. 9, article 834958, 2022.

[4] Q. M. Huang, J. Li, S. M. Liu, and G. Wang, "Experimental study on the adverse effect of gel fracturing fluid on gas sorption behavior for Illinois coal," *International Journal of Coal Science & Technology*, vol. 8, no. 6, pp. 1250–1261, 2021.

[5] T. Liu, B. Q. Lin, X. H. Fu, and A. Liu, "Mechanical criterion for coal and gas outburst: a perspective from multiphysics coupling," *International Journal of Coal Science & Technology*, vol. 8, no. 6, pp. 1423–1435, 2021.

[6] M. H. Yi, L. Wang, C. M. Hao, Q. Q. Liu, and Z. Y. Wang, "Method for designing the optimal sealing depth in methane drainage boreholes to realize efficient drainage," *International Journal of Coal Science & Technology*, vol. 8, no. 6, pp. 1400–1410, 2021.

[7] S. Y. Wu, *Coupling Motion Theory in Coal Seam and Its Application*, Science Press, Beijing, 2009.

[8] G. Z. Yin, M. H. Li, S. Z. Li, W. P. Li, J. W. Yao, and Q. G. Zhang, "Three-dimensional numerical simulation of gas extraction by borehole based on solid-gas coupling model of gas-bearing coal rock," *Journal of China Coal Society*, vol. 38, no. 4, pp. 535–541, 2013.

[9] Q. Q. Liu, Y. P. Cheng, W. Li, T. He, and W. Zhao, "Gas-solid coupling model of coal and gas in deep low-permeability first mining seam," *Chinese Journal of Rock Mechanics and Engineering*, vol. 34, no. S1, pp. 2749–2758, 2015.

[10] H. Zhang, J. Liu, and D. Elsworth, "How sorption-induced matrix deformation affects gas flow in coal seams: a new FE model," *International Journal of Rock Mechanics and Mining Sciences*, vol. 45, no. 8, pp. 1226–1236, 2008.

[11] B. Liang, X. P. Yuan, and W. J. Sun, "Coupling model and application of bedding gas drainage in this coal seam and seepage flow," *Journal of China University of Mining & Technology*, vol. 43, no. 2, pp. 208–213, 2014.

[12] B. Q. Lin, T. Liu, and W. Yang, "Establishment and application of coal seam multi-field coupling model based on dynamic diffusion," *Journal of China University of Mining & Technology*, vol. 47, no. 1, pp. 32–39, 2018.

[13] Y. Song, B. Jiang, C. T. Wei et al., "A review on the application of molecular dynamics to the study in coalbed methane geology," *Frontiers in Earth Science*, vol. 9, 2021.

[14] Y. Song, B. Jiang, M. Li, C. L. Hou, and S. C. Xu, "A review on pore-fractures in tectonically deformed coals," *Fuel*, vol. 278, article 118248, 2020.

[15] Q. Huang, B. Wu, Y. Liu, Z. Guo, G. Wang, and L. Sun, "Experimental and simulation investigations of the impact of polyacrylamide on CBM ad-/desorption," *Journal of Petroleum Science and Engineering*, vol. 208, article 109300, 2022.

[16] C. J. Fan, S. Li, M. K. Luo, W. Z. Du, and Z. H. Yang, "Coal and gas outburst dynamic system," *International Journal of Mining Science and Technology*, vol. 27, no. 1, pp. 49–55, 2017.

[17] C. L. Zhang, J. Xu, S. J. Peng, Q. X. Li, and F. Z. Yan, "Experimental study of drainage radius considering borehole interaction based on 3D monitoring of gas pressure in coal," *Fuel*, vol. 239, pp. 955–963, 2019.

[18] H. Lin, M. Huang, S. Li, C. Zhang, and L. Cheng, "Numerical simulation of influence of Langmuir adsorption constant on gas drainage radius of drilling in coal seam," *International Journal of Mining Science and Technology*, vol. 26, no. 3, pp. 377–382, 2016.

[19] W. Qin, J. Xu, G. Z. Hu, J. Gao, and G. Xu, "Measurement and simulation study on effective drainage radius of borehole along coal seam," *Energy Exploration & Exploitation*, vol. 37, no. 6, pp. 1657–1679, 2019.

[20] P. Zhao, L. Z. Xie, Z. C. Fan, L. Deng, and J. Liu, "Mutual interference of layer plane and natural fracture in the failure behavior of shale and the mechanism investigation," *Petroleum Science*, vol. 18, no. 2, pp. 618–640, 2021.

[21] W. Zhao, K. Wang, R. Zhang, H. Z. Dong, Z. Lou, and F. H. An, "Influence of combination forms of intact sub-layer and tectonically deformed sub-layer of coal on the gas drainage performance of boreholes: a numerical study," *International Journal of Coal Science & Technology*, vol. 7, no. 3, pp. 571–580, 2020.

[22] G. Bai, J. Su, Z. G. Zhang et al., "Effect of CO2 injection on CH4 desorption rate in poor permeability coal seams: An experimental study," *Energy*, vol. 238, article 121674, 2022.

[23] X. F. Liu, C. H. Liu, and G. Q. Liu, "Dynamic behavior of coalbed methane flow along the annulus of single-phase production," *International Journal of Coal Science & Technology*, vol. 6, no. 4, pp. 547–555, 2019.

[24] C. J. Fan, S. Li, M. K. Luo, H. Z. Yang, H. H. Zhang, and S. Wang, "Numerical simulation of deep coalbed methane drainage based on fluid-solid-heat coupling," *Journal of China Coal Society*, vol. 41, no. 12, pp. 3076–3085, 2016.

[25] Y. Fan, C. Deng, X. Zhang, F. Li, X. Wang, and L. Qiao, "Numerical study of CO_2-enhanced coalbed methane recovery," *International Journal of Greenhouse Gas Control*, vol. 76, pp. 12–23, 2018.

[26] P. Zhao, L. Xie, B. He, and J. Liu, "Anisotropic permeability influencing the performance of free CH4 and free CO2 during the process of CO2 sequestration and enhanced gas recovery (CS-EGR) from shale," *ACS Sustainable Chemistry & Engineering*, vol. 9, no. 2, pp. 914–926, 2021.

[27] B. J. Huo, X. D. Jing, C. J. Fan, and Y. L. Han, "Numerical investigation of flue gas injection enhanced underground coal seam gas drainage," *Energy Science & Engineering*, vol. 7, no. 6, pp. 3204–3219, 2019.

[28] C. J. Fan, D. Elsworth, S. Li et al., "Modelling and optimization of enhanced coalbed methane recovery using CO_2/N_2 mixtures," *Fuel*, vol. 253, pp. 1114–1129, 2019.

[29] S. Li, C. Fan, J. Han, M. K. Luo, Z. H. Yang, and B. J. Huo, "A fully coupled ther-mal-hydraulic-mechanical model with two-phase flow for coalbed methane extraction," *Journal of Natural Gas Science and Engi-neering*, vol. 33, pp. 324–336, 2016.

[30] C. J. Fan, D. Elsworth, S. Li, L. J. Zhou, Z. H. Yang, and Y. Song, "Thermo-hydro-mechanical-chemical couplings controlling CH_4 production and CO_2 sequestration in enhanced coalbed methane recovery," *Energy*, vol. 173, pp. 1054–1077, 2019.

[31] Y. P. Fan, L. Y. Shu, Z. G. Huo, J. W. Hao, and Y. Li, "Numerical simulation research on hydraulic fracturing promoting coalbed methane extraction," *Shock and Vibration*, vol. 2021, Article ID 3269592, 12 pages, 2021.

[32] Q. Wang, Z. H. Jiang, B. Jiang, H. K. Gao, Y. B. Huang, and P. Zhang, "Research on an automatic roadway formation method in deep mining areas by roof cutting with high-strength boltgrouting," *International Journal of Rock Mechanics and Mining Sciences*, vol. 128, article 104264, 2020.

[33] C. J. Fan, L. Yang, G. Wang, Q. M. Huang, X. Fu, and H. O. Wen, "Investigation on coal skeleton deformation in CO2 injection enhanced CH4 drainage from underground coal seam," *Frontiers in Earth Science*, vol. 9, 2021.